Special Review

Review

Human Characteristics Models for Automobile Design

Toshihiro Wakita

Report received on Nov. 21, 2017

ABSTRACT To develop safe and comfortable automobiles, their design must reflect human characteristics. Human characteristics modeling is an important technology for developing a high-quality vehicle that reflects human characteristics effectively and efficiently. Development of these models can be categorized into two basic approaches: physical models and statistical models. Each approach has advantages and disadvantages. In this paper, four studies of different automobile human characteristics models are reviewed and discussed: (1) A sound quality evaluation method was developed using a psychophysical model. (2) Information equipment operation behaviors were analyzed using a cognitive model, and indices were developed for application to human-machine interface design. (3) A drowsiness detection method was proposed using a brain function model and the results of functional magnetic resonance imaging experiments. (4) Individual driver behavior was modeled using both physical and statistical models, and the results for each model were compared and discussed.

KEYWORDS Human Characteristics Modeling, Sound Quality, Operation Behavior, Drowsiness Detection, Driving Behavior, Automobile Design

1. Introduction

Humans need to drive automobiles without accidents, most of which are caused by human error. Also, people want to be comfortable in automobiles, which means that the qualities of the automobile must be pleasing to human senses. Therefore, to develop safe and comfortable automobiles, automobile design must reflect human characteristics.

Many studies have evaluated human characteristics for automobiles. In the 1990s, as basic automobile performance had matured and a booming economy continued, consumers demanded automotive products with higher quality. For instance, the designs of body color, engine sound, seat textile, interior odor, and vehicle motion became more important. Consequently, human senses (for sight,[1] hearing,[2] tactile sensation,[3] smell,[4] and motion[5]) were extensively studied. In the 2000s, the focus shifted to information and communication technologies, and cell phones and car navigation systems became popular. Some accidents occurred when drivers used this equipment while operating their vehicles. To mitigate negative impacts of this equipment, the human-machine interface[6] and mental workload of drivers[7] were widely studied. In the 2010s, with the aging of society and the progress of artificial intelligence technology, active safety systems and automated driving systems are being developed. Accordingly, the driving behavior[8] and the cooperation between man and machine[9] are intensively studied.

Thus, it has become necessary to clarify various human characteristics to address the changing needs of these times.

2. Human Characteristics Models

2. 1 Reflecting Human Characteristics in Automobile Design

To reflect human characteristics, designers have typically employed the following prototyping method:

(i) Design the first specification.
(ii) Create a prototype.
(iii) Evaluate the prototype using human evaluators.
(iv) Change the specification according to the evaluation result.
(v) Repeat steps 2, 3, and 4.

However, this process is not efficient for the following reasons:

- **Reproducibility of Evaluation:** Humans sometimes sense the same stimuli differently and behave differently in the same situation. For example, human evaluators' results for the same engine sound often vary. They are affected by the order in which evaluations are performed, evaluator's physical condition, and the duration of the testing. To compensate for these artifacts, the evaluation should be repeated many times, which wastes time and effort.
- **Inter-evaluator Agreement:** Human characteristics differ depending on the person. For example, it is not unusual for two human evaluators to have different results. However, it is difficult to know which result is a better representation of the parent population. To resolve this problem, a number of human evaluators should participate in the evaluation, which again is inefficient.
- **Prototyping:** To execute the process, construction of a prototype is essential. However, prototyping consumes time and effort. Especially, the building of hardware prototypes, such as engines, steering wheels, and vehicle bodies, requires much time and money.

In an attempt to resolve the above problems, mathematical models of human characteristics can be developed. This model-based method offers the following advantages:

- The evaluation can be done rapidly, and human evaluators are minimized or eliminated.
- The evaluation result has a high degree of reproducibility.
- As the relationship between the specification and the evaluation result is clear, the designer can change the specification without prototyping.

Today, the development period for vehicles is becoming shorter because of rapidly changing market needs and strong competition between car manufacturers. As a result, human characteristics modeling has become an important technology for developing high-quality vehicles that reflect human characteristics.

2. 2 Human Characteristics Models for Vehicles

Human characteristics models can be classified into two approaches to model development: physical modeling and statistical modeling. In the first approach, a physical model is used to describe the human characteristics. The physical models commonly used are psychophysical models, cognitive models, transfer function of control theory, biological models, and brain functional models. In the second approach, human characteristics are described using statistical models. The models often use basic statistics, factor analysis, discrimination analysis, regression analysis, support vector machines, and convolutional neural networks. These two approaches are further elaborated below.

The advantages of the physical modeling approach are as follows. If a physical model explains the targeted characteristics well and the model is well-established, the design process is very efficient. Such physical models have been established for many situations and people, eliminating the need to design a new model or collect new experimental data. Furthermore, since the physical meaning of the model is explicit, the capabilities and limits of the model are clear and easy to apply to the design. On the other hand, it is generally difficult to increase the accuracy of a physical model and expand its range of applicability. For example, the modeling of driving behaviors can be used to describe driving behavior linearly, although actual human behavior is usually nonlinear.

In contrast, the advantage of the statistical modeling approach is that physical knowledge about human characteristics is not necessary if sufficient measurements are available. One difficulty is that it requires many measurements. Although recently it has become relatively easy to obtain large quantities of data, collecting the desired data precisely requires much effort. Another difficulty is model selection. Normally, the true model structure cannot be known. If the selected statistical model is more complex than the true model, the generalization ability to effectively work on unknown data as well as data used at the time of experiment is sometimes degraded.[10] To compensate for this weakness, cross-validation tests and various criteria for model selection have been proposed.

To model individual driver characteristics, the modeling approach needs to be tailored based on the properties of the targeted human characteristics and relevant automobile component or system being designed. In this paper, four studies using automobile human characteristics models are reviewed and discussed to illustrate various aspects of model selection and application.

3. Sound Quality Evaluation: Psychophysical Model[2]

3. 1 Background

Demand for comfort in the vehicle passenger compartment has recently increased as the quality of passenger cars continues to improve. To make the compartment comfortable, not just the noise level but the noise type must be considered. One such example is rumble noise, which is an intermittent turbid engine noise. This rumble noise is unpleasant to passengers even if the noise level itself is low.

Previous studies have shown that rumble noise has the following characteristics:[11,12]

- Rumble noise is generated at an engine speed of around 3000 rpm during acceleration.
- The generating frequency band is approximately from 100 to 600 Hz.
- Sound pressure amplitude significantly fluctuates with a period of two engine revolutions (**Fig. 1**).

However, the conventional evaluation methods used in these studies failed to correlate rumble with the capabilities of human hearing. Specifically, the amplitude modulation obtained from the signal of 100 Hz to 600 Hz does not match human auditory perception. In this section, an evaluation method using a psychophysical model is reviewed.

3. 2 Modeling of Rumble Evaluation

The human hearing organ is composed of a number of band-pass filters connected in parallel. A person cannot distinguish multiple sounds with different frequencies within the pass bandwidth of the filter, and the sounds are heard as just one composite sound. This characteristic is called critical band,[13] and it is a common concept in hearing psychophysics. Thus, a person hears multiple components of n/2 order (n = 1, 2, ...) of engine revolutions in a critical band as one amplitude-modulated sound with a period of two engine revolutions (**Fig. 2**).

The above considerations were used in modeling the rumble evaluation by humans, as shown in **Fig. 3**. In the model, sound reaching the ears of a person is divided into many bands corresponding to critical bands, followed by detection of the amplitude modulation of sound in each band. The amplitude modulation is then evaluated and a partial rumble evaluation is determined for each band. Lastly, the partial rumble evaluations for each band are integrated into one rumble evaluation for the entire sound.

3. 3 Analysis of Rumble Noise

On the basis of the model of rumble evaluation, many kinds of rumble noises in the vehicle passenger compartment were analyzed to find out how amplitude modulation was perceived as rumble. **Figure 4** shows an example of rumble noise where the amplitude modulation with a period of two engine revolutions is excessive. This figure represents (a) the frequency components of noise in the vehicle passenger compartment, (b) the waveform of the noise restricted to a critical band and its envelope, and (c) the frequency components of the envelope. This type of noise gives a strong sense of rumble to human ears, and the model confirmed that a person perceives the amplitude

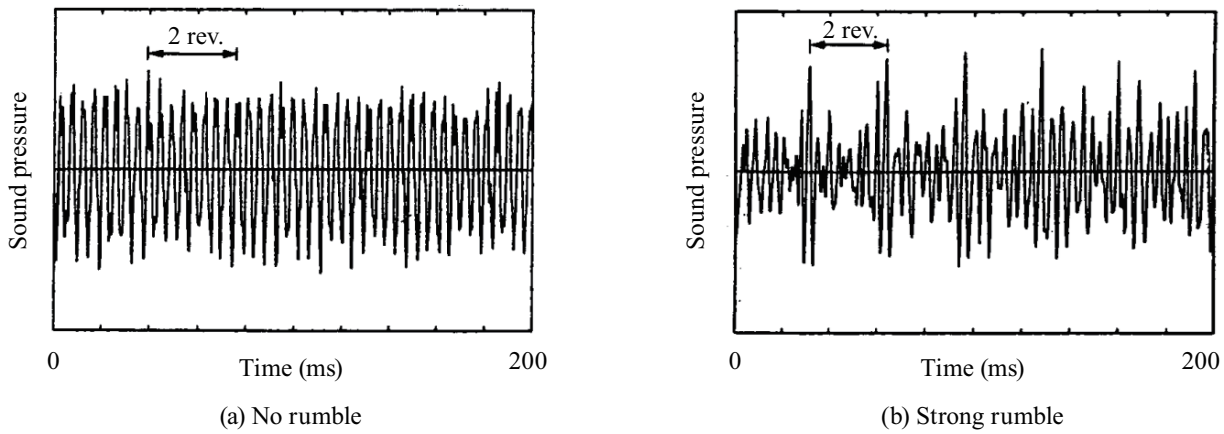

Fig. 1 Waveform of noise in vehicle passenger compartment.

modulation with a period of two engine revolutions as rumble. The period of two engine revolutions is hereafter called the principal rumble period, and the frequency component of the envelope containing the principal rumble period is called the principal rumble component.

The model identified various types of amplitude modulation. In some rumble noises, the degree of modulation is low and the rumble is perceived to be weak. In other rumble noises, the modulation period of one engine revolution is dominant and the rumble is also perceived to be weak. Based on these results, it was found that the evaluation of rumble is influenced not only by the principal rumble component but also by various features of amplitude modulation.

3. 4 Quantification of a Sense of Rumble by Synthesized Noise

In the next stage, sensory evaluation tests were conducted to quantify the relationship between the feature of amplitude modulation and the sense of rumble. First, the relationship between the amplitude of the principal rumble component and the sense of rumble was studied. Synthesized sounds were generated by varying the number of harmonics n constituting the synthesized noise and the amplitude A_i of each harmonic in Eq. (1).

$$\sum_{i=1}^{n} A_i \sin 2\pi \left(f_0 + \left(i - \frac{n+1}{2} \right) f_a \right) t \ , \tag{1}$$

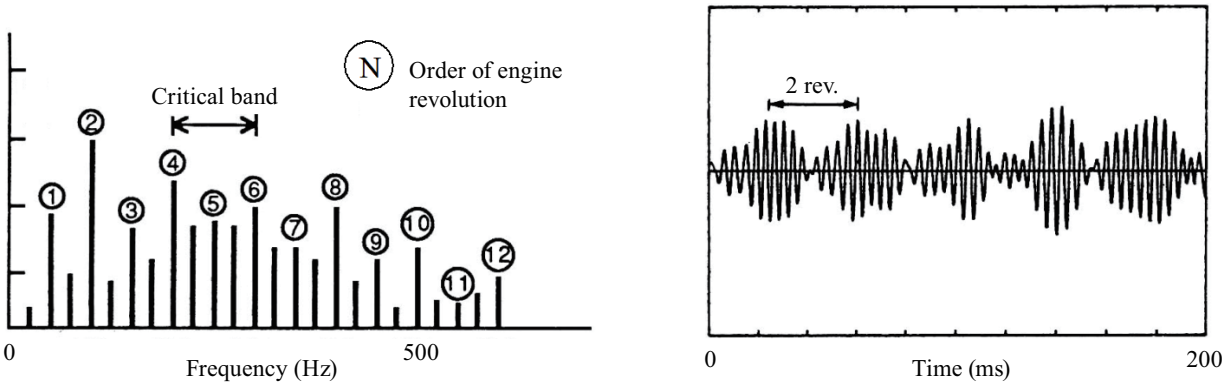

(a) Frequency spectrum of a sound

(b) Waveform in which the sound is limited to the critical band indicated in (a)

Fig. 2 Mechanism of generating rumble.

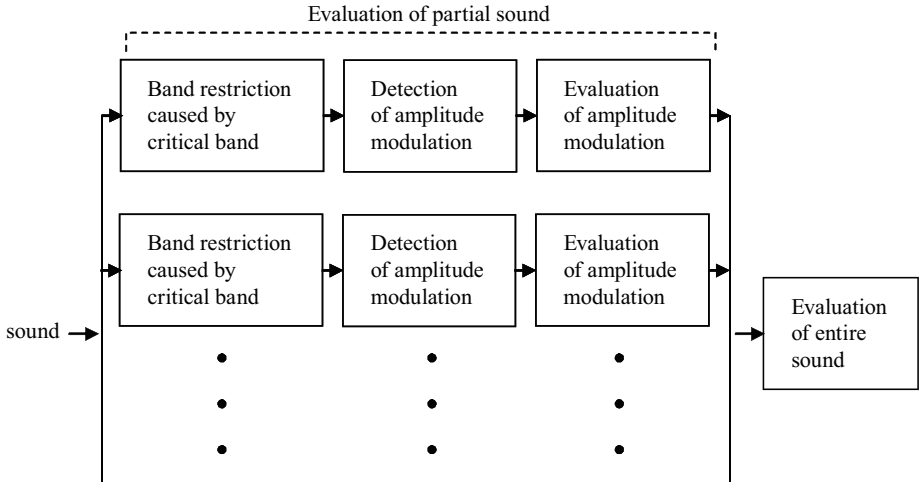

Fig. 3 Rumble evaluation model for human hearing.

where f_0 = 250 Hz (center frequency) and f_a = 25 Hz (modulation frequency). Each harmonic corresponds to the noise component of n/2 order of engine revolutions at 3000 rpm. Then, 12 subjects evaluated the sense of rumble in the test sounds. The test results (**Fig. 5**) showed that the sense of rumble has a strong correlation with the amplitude of the principal rumble component. In other words, the sense of rumble could be quantified using the amplitude of the principal rumble components.

Next, the influence of modulation degree was investigated. Subjects evaluated sounds with various degrees of modulation. As a result, it was found that even if the amplitudes of the principal rumble components are the same, the sense of rumble became weak as the degree of modulation decreased. The results are shown in **Fig. 6**. The rumble correction coefficient represents the extent to which the sense of rumble was reduced with respect to that of the sound according to the degree of modulation.

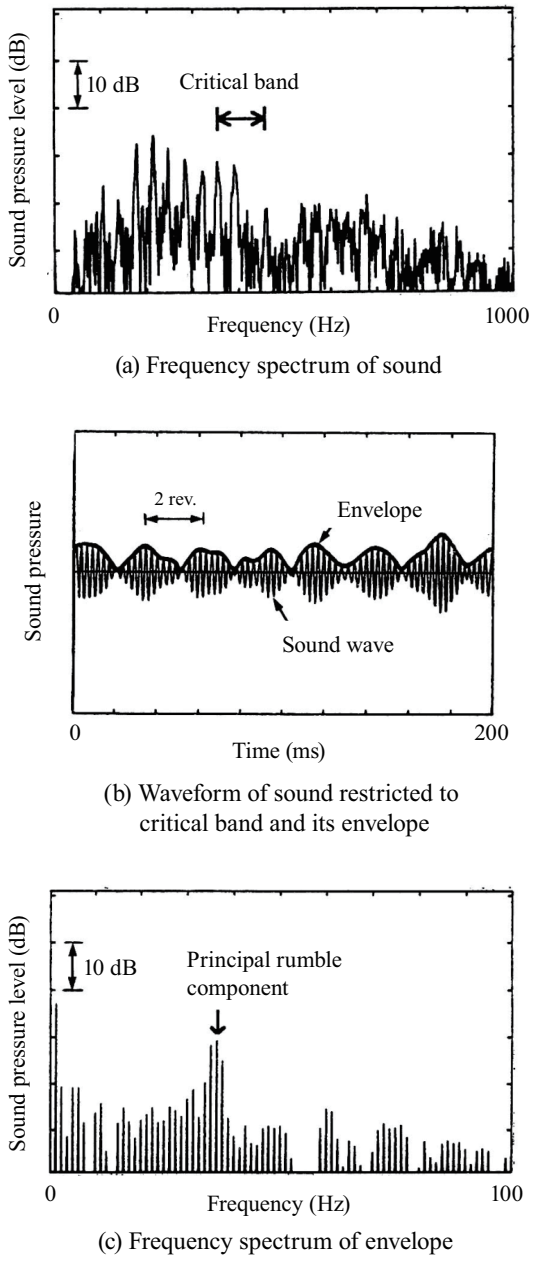

Fig. 4 An example of large amplitude modulation having a period of two engine revolutions.

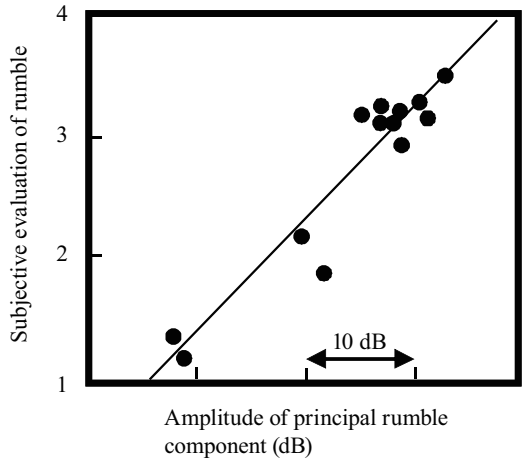

Fig. 5 Relationship between the amplitude of the principal rumble component and the subjective evaluation. The line represents a regression line.

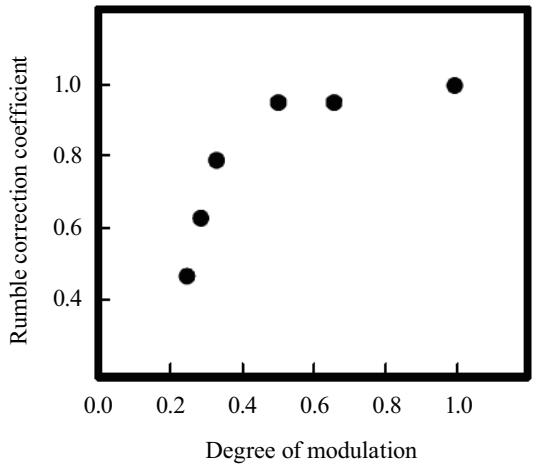

Fig. 6 Relationship between the degree of modulation and the rumble correction coefficient. 'Rumble correction coefficient' represents the extent to which the sense of rumble was reduced with respect to that of the sound with the degree of modulation 1.

By conducting similar experiments, rumble correction coefficients for the amplitude of the envelope of the first-order component of engine revolution and the principal rumble period were obtained.

3. 5 Objective Evaluation Model of Rumble

An objective evaluation model was proposed on the basis of the above relationships (**Fig. 7**). The model divides sound into critical bands, detects the amplitude modulation in each band, and measures the amplitude of the principal rumble component. Next, rumble correction coefficients are obtained based on the degree of modulation, the amplitude of the envelope of the first-order component of engine revolution, and the principal rumble period. Then, the value obtained by multiplying the rumble correction coefficients and the amplitude of the principal rumble component is set as a partial rumble evaluation for each band. Finally, the maximum value of the partial evaluation values is taken as the objective evaluation of the whole sound.

Figure 8 shows the relationship between the objective and subjective evaluations of actual vehicle sounds. Using the physical model of human hearing (critical band), an objective evaluation model that produced good matching with the subjective evaluations was obtained.

4. Information Equipment Operation: Cognitive Model[14]

4. 1 Background

In recent years, there has been an enormous growth in the popularity of in-vehicle information systems, including vehicle navigation systems. This trend will most likely continue as intelligent transport systems and information technologies advance further. Because drivers use these systems while controlling a vehicle, the systems must be safe to use as well as convenient. Implementing in-vehicle human-machine interfaces that are both safe and convenient requires clarification of the following two items:

- Indices for objectively evaluating in-vehicle information system usability and safety.
- Relationships between evaluation indices and human-machine interface design specifications.

4. 2 Evaluation Indices

Usability

Various measures have been proposed as possible indices for evaluating usability. These include the operation time, the number of operations, task

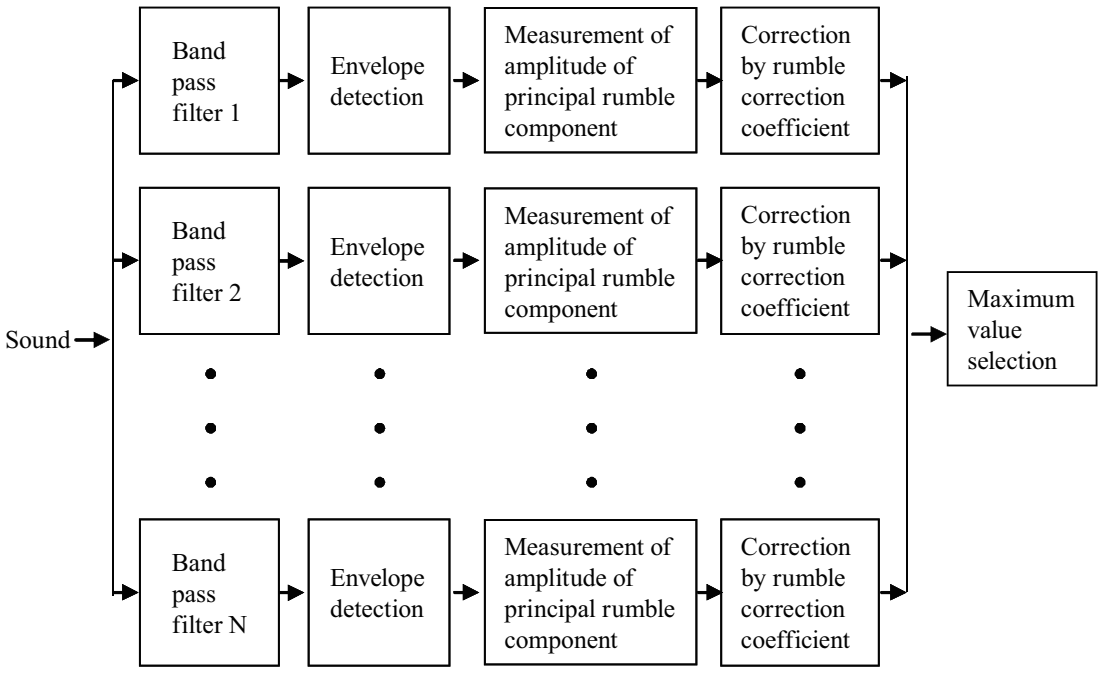

Fig. 7 Objective evaluation model of rumble.

achievement ratio, and the "beginner-to-designer" manipulation time ratio.[15] The total task time was selected for evaluation of in-vehicle information systems, because it is important to accomplish tasks as quickly as possible for drivers driving a vehicle.

Safety

For visual interfaces, the total glance time has been proposed as a safety evaluation index.[16-18] This index cannot, however, be applied to auditory interfaces, in that they do not involve any visual recognition aspect. In addition, the subjective evaluation proposed in the NASA task load index (NASA-TLX)[19] and other indices have problems with the reproducibility and reliability of the evaluation. Meanwhile, it has been reported that most traffic accidents attributable to the use of in-vehicle information systems (mobile phones: 80%,[20] vehicle navigation systems: 60%[21]) were rear-end collisions. Most rear-end collisions are caused by delayed brake reaction to a situation change in front of the vehicle. For this reason, the ratio of the delayed reaction was selected as the safety evaluation index. Using a method proposed previously,[22] this safety evaluation index could be measured objectively.

4. 3 Visual Interface

Visual and auditory interfaces are mainly used as the human-machine interface for information equipment. In this section, a method in which the evaluation indices for visual interfaces was developed using a cognitive model is reviewed.

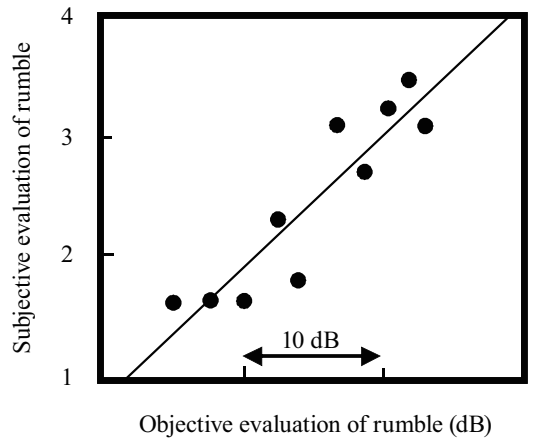

Fig. 8 Relationship between the objective evaluation and the subjective evaluation of actual vehicle sounds in the vehicle passenger compartment. The line represents a regression line.

4. 3. 1 Experiment

To examine driver behavior during system operation, hand movement, eye movement, and the system screen were video-recorded while test subjects were parking and driving. Experimental conditions were as follows:

- **Equipment:** Car navigation system, touch-pad type
- **Task:** Entry of four, six, or eight different destinations requiring two to six operations each; the operation sequence was explained by experimenter prior to the experiment.
- **Driving Status:** Driving 50 km/h on a straight track and parking. To control the driving task, subjects were instructed to keep to the center of the lane and monitor the on-off status of three LEDs mounted at the front of the car.
- **Test Subjects:** Six males (three in their 30s and three in their 50s)
- **Number of Trials:** Four trials each of 4, 6, and 8 destinations (total of 12 trials for each subject)

4. 3. 2 Operation Analysis

Examples of the operation behavior are shown in **Fig. 9**. To analyze and model the operations, the cognitive keystroke-level model (KLM)[23] was used. In this model, human operations are expressed as a series of operators to accomplish a goal. The types of operators are keystroke, pointing, hand moving, mental preparation, and system response.

Based on the model, it was assumed that operation of the navigation system while parking included three phases:

- Phase M (mental preparation): Look at navigation system display, read and search menu items, and decide operation.
- Phase H (hand homing): Move hand to menu location and touch menu option.
- Phase W (waiting for next operation): Wait and prepare for the next operation.

Phases M', H', and W' represent the same activities while driving.

Visual behaviors were different between parking and driving conditions. A driver could look at the navigation display continuously while parking, but he had to look at either the road or the display while

driving. The driver looked at the display to read the menu in phase M' and to position his hand in phase H'. In phase M', the glance was sometimes divided into multiple glances. In phase W', the driver did not look at the display but looked continuously at the road.

By analyzing these visual behaviors, the following properties were found:

- Operation time t_s, representing the duration of phases M and H, was linearly correlated to the number of menu options m.

$$t_s = A \cdot m + B \,, \tag{2}$$

where A and B are constants.

- Glance time e_g, representing the total time when the driver is not looking at the road, is the sum of fixation time e_i, representing the duration that eyes look at the display, and the constant T_t.

$$e_g = e_i + T_t \tag{3}$$

T_t corresponds to the line-of-sight eye movement time (i.e., the time the eye takes to shift focus from one location to another) and is around 0.23 s.

- The sum of fixation time in phase M' + H' while driving, t_i, is equal to the sum of operation time in phase M + H while parking, t_s.

$$t_i = t_s \tag{4}$$

- The sum of glance time in phase M' + H' while driving, t_g, is linearly proportional to the number of glances per operation while driving, n_g.

$$t_g = C \cdot n_g + D \,, \tag{5}$$

where C and D are constants. t_g can also be described by the following equation.

$$t_g = n_g T_t + t_i \tag{6}$$

- From Eqs. (5) and (6), the number of glances per

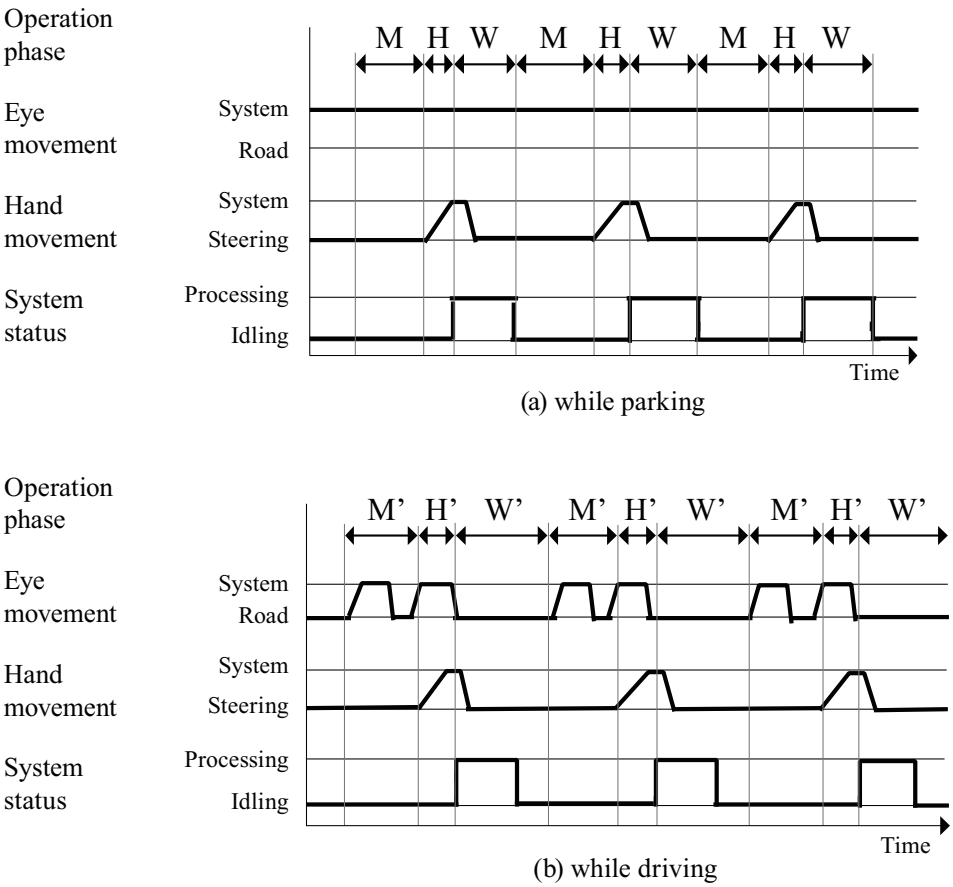

Fig. 9 Example of operation behavior.

operation while driving, n_g, was calculated as follows:

$$n_g = \frac{A \cdot m + B - D}{C - T_t} \quad , \tag{7}$$

where C and D are constants.

- The total time during which the driver is looking at the road between the divided glance, e_f, is about 0.7 s.
- The waiting time in phase W was almost same as the system response time t_r.

4. 3. 3 Calculating the Evaluation Index for Visual Interfaces

Prediction of Total Task Time

Based on the properties described above, a model of navigation system operation while driving was constructed (**Fig. 10**). Using the model, the total task time T, which is an index of usability, can be calculated as follows:

$$\begin{aligned} T &= n_o\left(t_g + \left(n_g - 1\right)e_f\right) + n_o t_r \\ &= n_o\left(\frac{C \cdot A \cdot m + C \cdot B - D \cdot T_t}{C - T_i}\right. \\ &\quad \left. + \left(\frac{A \cdot m + B - C}{C - T_i} - 1\right)e_f\right) + n_o t_r \, . \end{aligned} \tag{8}$$

Finally, the total glance time T_G can be calculated as follows:

$$\begin{aligned} T_G &= n_o \cdot t_g \\ &= n_o \cdot \frac{C \cdot A \cdot m + C \cdot B - D \cdot T_t}{C - T_t} \, , \end{aligned} \tag{9}$$

where n_o is the number of operations; m is the number of menu options; t_r is the system response time; A, B, C, D, and T_t are constants.

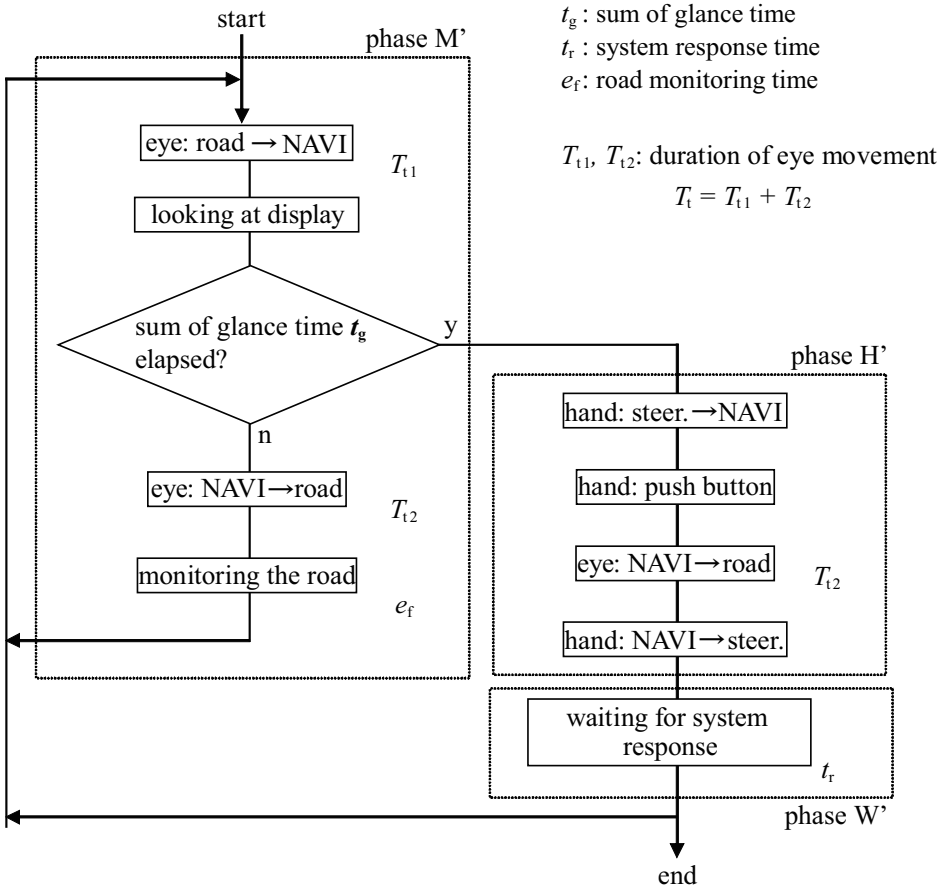

Fig. 10 Visual operation model while driving.

Figure 11 shows the relationship between the predicted T_G and the T_G measured during actual navigation system operation. As shown in this figure, the metrics for usability calculated by this operating model were approximately the same as the measured data. The correlation coefficient was 0.96, and the average root mean square error was 0.7 s.

Prediction of the Ratio of Delayed Reaction

The ratio of delayed reaction is a calculated safety index. In this study, the delayed reaction was defined as a reaction whose reaction time was three standard deviations (3σ) or longer than the average reaction time μ while a driver continuously looks at the road. σ represents the standard deviation of reaction time.

While driving, assuming that a driver looks at the display during time period T_1 and looks at the road during time period T_2, the average ratio of delayed reaction is calculated as follows:

$$\frac{T_1 + R_f T_2}{T_1 + T_2}, \tag{10}$$

where R_f is the ratio of delayed reaction when a driver continuously looks at the road. Then, the ratio of delayed reaction R for a visual interface can be calculated as follows:

$$R = \frac{T_G + R_f (T - T_G)}{T}. \tag{11}$$

4. 4 Example Application of Usability Evaluation

Similar analyses and modeling were also carried out for auditory interfaces.

Auditory and visual interfaces were compared using an information search task. **Figure 12** shows the results of the comparison. In this chart, the horizontal axis represents the safety index, that is, the ratio of delayed reaction, while the vertical axis corresponds to the usability index, that is, the total task time. The results of the comparison quantitatively prove that the auditory interface is safer than the visual interface and that the use of a word enumeration or fixed-phrase protocol can realize auditory interfaces that are more convenient than visual interfaces.

As described above, by using the keystroke-level model, it was possible to create a model that can evaluate usability and safety and clearly relates to design specifications.

5. Drowsiness Detection: Brain Function Model[24,25]

5. 1 Background

Drowsy driving is one of the main causes of traffic accidents, and delayed reactions caused by drowsiness can result in severe car crashes. Onboard drowsy-driver detection systems with sensors to measure drowsiness would be effective for preventing such accidents. The key technology for such systems depends on finding a drowsiness index that can estimate the driver reaction delay precisely and that also can be measured onboard.

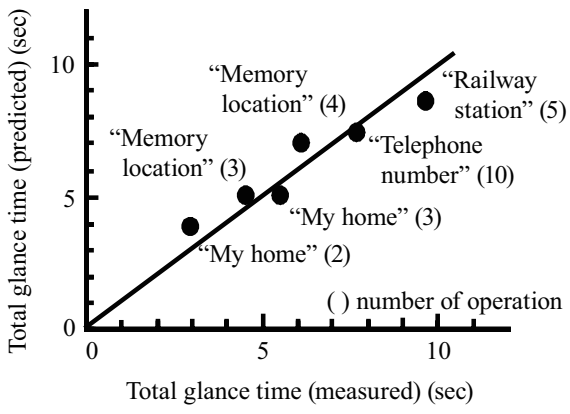

Fig. 11 Prediction of the total glance time. The line represents a regression line.

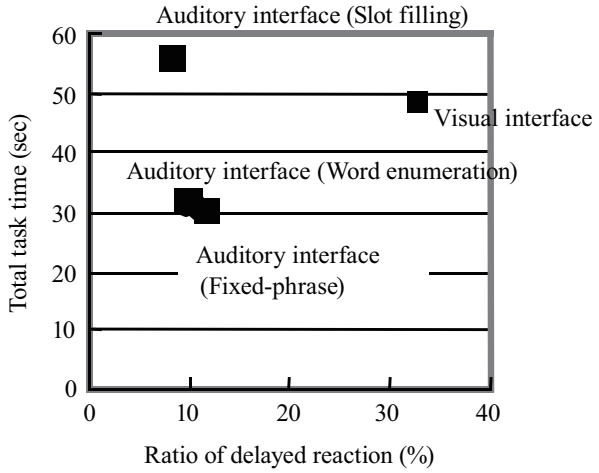

Fig. 12 Comparison of auditory interface and visual interface.

Although many studies were carried out to find such an index,[26, 27] no precise index was known at the time of the study. Conventional research had focused on the correlation of data obtained by experiment but had not considered the mechanism of drowsiness. As a result, sufficient accuracy could not be obtained.

The study reviewed here was carried out in two steps. First, delayed reactions caused by drowsiness were analyzed using functional magnetic resonance imaging (fMRI) and the neurophysiological mechanism was explored.[24] Second, based on the mechanism, a drowsiness index was proposed.[25]

5. 2 Analysis of Delayed Reaction Caused by Drowsiness

As the first step, fMRI was used to investigate neural mechanisms of the reaction delay in a drowsy state. Twenty healthy subjects performed an auditory reaction task (**Fig. 13**) continuously for about 75 min during fMRI measurements. During the task, the shortest reaction time of any subject was about 300 ms. Of the 20 participants, 19 were unable to respond to the auditory stimulus during several trials, although the inter-stimulus interval was sufficiently long to respond. In other words, in these trials, the reaction time was infinite. This large variation of reaction times in one experiment suggests that the arousal level of subjects differed greatly between the awake and asleep stages.

The control center for awake and asleep stages is known to reside in the brainstem.[28] Therefore, brain activity in the brainstem in trials with short and long reaction times was compared (**Fig. 14**). In the figure's upper panel, black squares show positions where brain activation in go-without-warning trials with a short reaction time was significantly greater than that at long reaction times (paired t-test $p < 0.05$). This upper region where the black squares are clustered

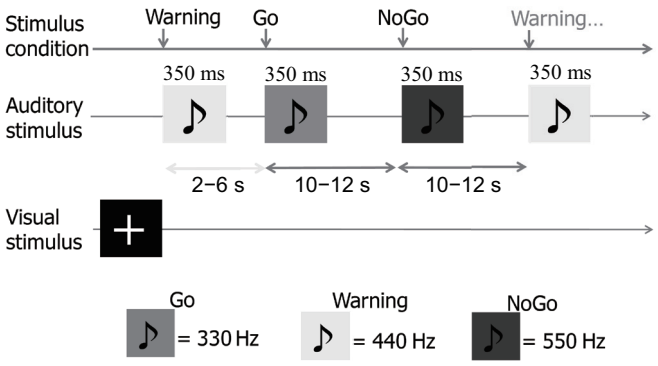

Fig. 13 Time course of auditory and visual stimulus presenting for fMRI measurements. There are four kinds of auditory stimuli: GO without warning, NOGO without warning, GO with warning, and NOGO with warning.

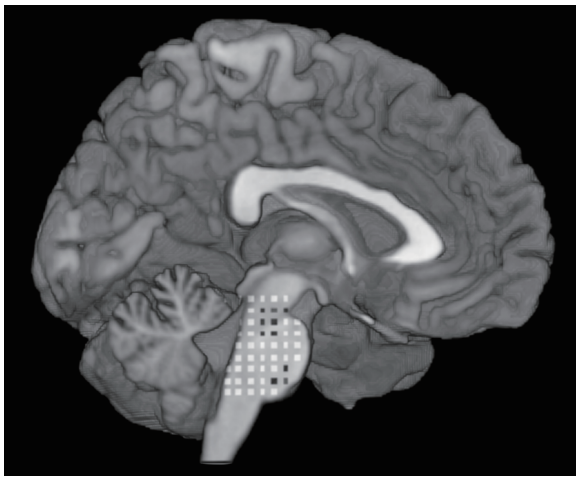

(a) The squares indicate the brain activation in the brainstem of the Go without warning trials. The black squares indicate the position on which the activation of the trial with the short reaction time was statistically significantly higher (paired t-test $p < 0.05$) than that with the long reaction time.

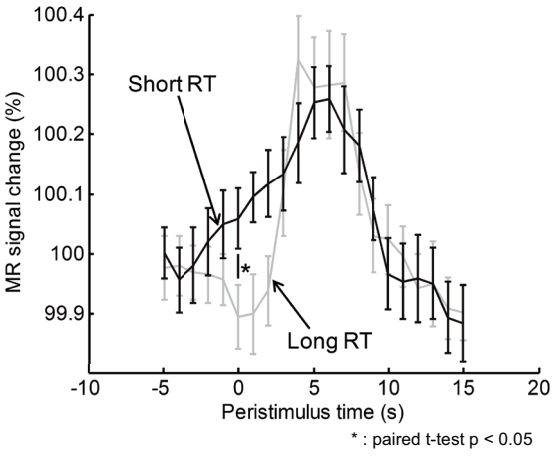

(b) The eristimulus time course of the brain activity in the brainstem at the MNI coordinates (2, −26, −26). Black and gray line indicate the time course of the short reaction time trials (Short RT) and that of the long reaction time trials (Long RT) respectively.

Fig. 14 The brain imaging result and the peristimulus time course of the brain activity.

is called the brainstem reticular formation and is known to be related to attention.[29] The lower panel shows respective peristimulus time courses of brain activity for the black squares in the upper panel. The results suggest that the delayed reaction caused by drowsiness is related to activity in the brainstem reticular formation.

5. 3 Drowsiness Index

Because the activity of the brainstem reticular formation is difficult to observe directly, it is inappropriate as a drowsiness index. Therefore, a way to observe this activity indirectly, from the outside was examined. In the brainstem reticular formation, activity of the omnipause neurons is affected by arousal signals, and these neurons in turn affect saccade eye movements (**Fig. 15**).[30] Therefore, an experiment to measure eye movements was carried out. Fourteen subjects sat on a dismounted car seat in front of an LCD monitor and were instructed to fixate on a visual target and depress a pedal in reaction to an auditory stimulus. Their eye movements were measured using electrooculography.

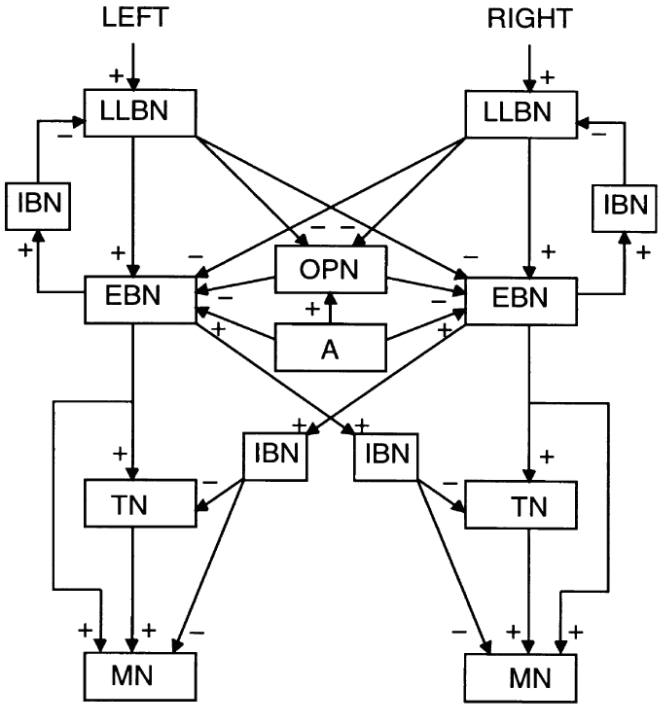

Fig. 15 Neural model of the saccade generator in the reticular formation. Omni pause neurons (OPN) is affected by arousal signal (A) and inhibit motor neurons (MN) through excitatory burst neurons (EBN). TN, IBN, LLBN represent tonic neurons, inhibitory burst neurons, and long-lead burst neurons, respectively.

Figure 16 shows examples of horizontal eye movements during the 5 s before stimulus presentation. Each column shows results from a different subject. The upper row is the results for observation of stable fixations. The lower row is the results for stimulus response, in which slow and sinusoidal-like oscillatory slow eye movements (SEM) appeared before the stimulus onset.

Figure 17 shows the times for reaction to auditory stimulus in the absence and presence of SEM. The reaction times are clearly different depending on the occurrence of SEM ($p < 0.001$, one-tailed paired t-test).

Based on the above results, a method to predict reaction delay by SEM occurrence was developed. The detection performance was compared with various conventional detection methods, as shown in **Fig. 18**. The SEM method had the highest detection rate and the lowest false detection rate. Thus, by using the neural functional model, a more accurate index for drowsiness was found.

6. Individual Driver Behavior: Statistical Model[31]

6. 1 Background

With increased emphasis being placed on the practicality and safety of vehicles, the recognition of driver-specific behavior has become much more important. The ability to recognize a driver and his or her driving behavior could form the basis of many applications, such as the ability to detect the driver becoming inattentive, the customization of vehicle functions to suit a driver's personal preferences, driver authentication for security purposes, and human-machine cooperative driving. A key technology for realizing these advances is human behavior signal processing, which involves the processing and recognition of human behavior signals, such as operation of the accelerator pedal. In this section, driver identification models based on such behavior signals is reviewed.

Driving behaviors are components of a cyclic process, as described below and illustrated in **Fig. 19**.

(i) The driver recognizes the road environment, including, for example, the road layout and the headway distance from the vehicle-in-front.

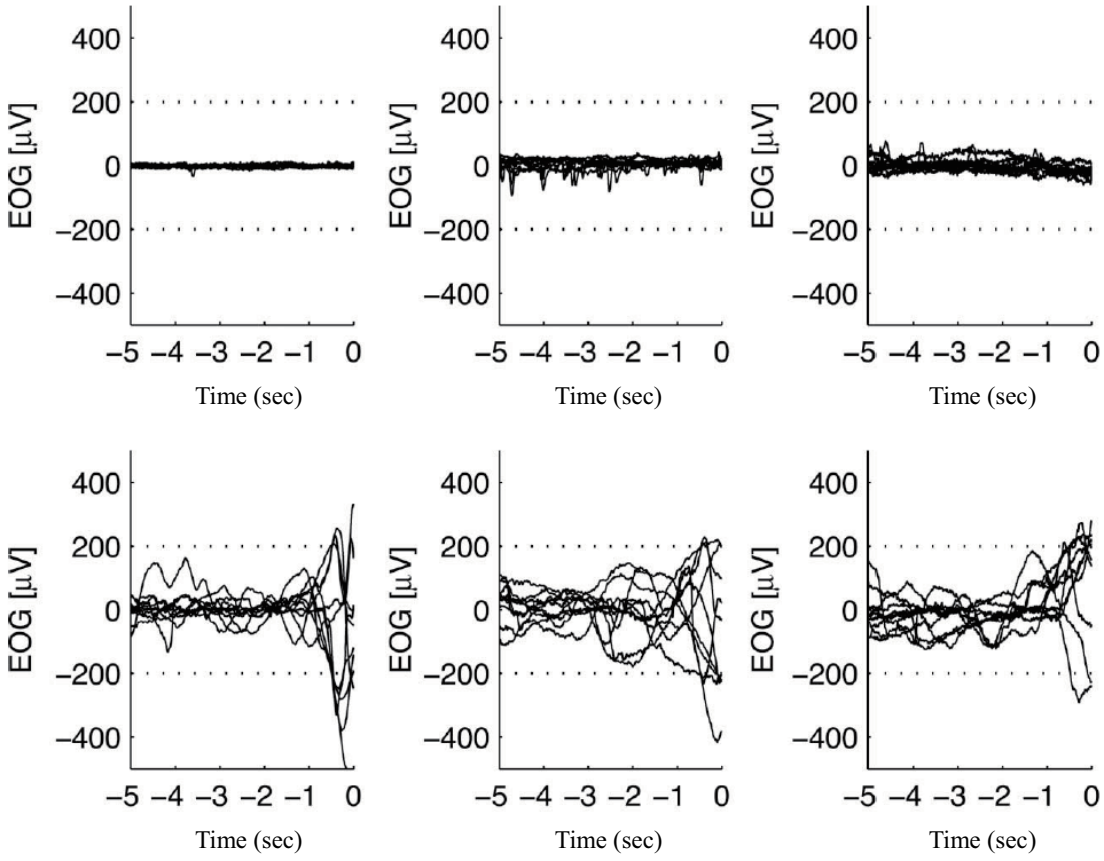

Fig. 16 Examples of horizontal eye movement for 5 sec before the stimulus presentation. Each column shows results from a different participant. The upper row is the results that stable fixations were observed. The lower row is the results that slow and sinusoidal-like oscillatory eye movements (SEM: Slow Eye Movement) appeared before the stimulus onset. The eye movements were measured using EOG (Electro-oculogram).

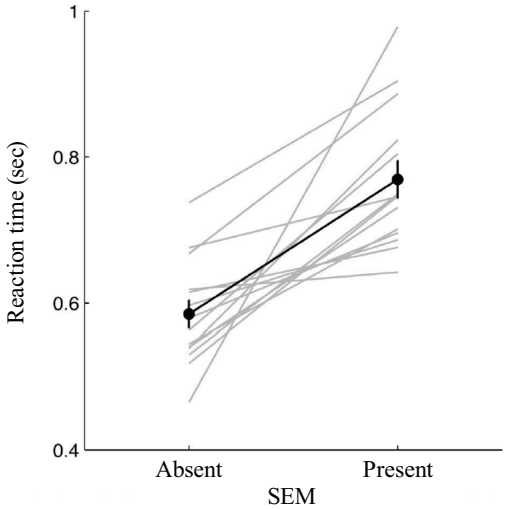

Fig. 17 Reaction times to the auditory stimulus in the absence and presence of slow eye movement (SEM). The black line indicates the mean reaction time for all subjects and the thin grey lines indicate mean reaction times for individual subjects. The error bars represent the standard error of the mean.

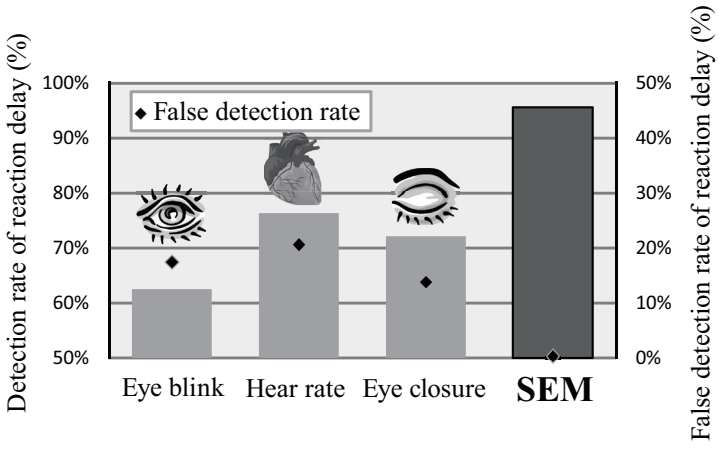

Fig. 18 Comparison of drowsy indexes. The bars represent the detection rate of reaction delays and the points represent the false detection rate of reaction delays.

(ii) The driver determines the action that he or she should take, such as accelerating, braking, and/or steering.
(iii) The driver operates the accelerator pedal, brake pedal, and/or steering wheel.
(iv) The vehicle status (e.g., velocity and yaw rate) changes according to the driver's operation of vehicle controls.
(v) The road environment (e.g., headway distance from the vehicle-in-front) changes according to the vehicle status.

The most elementary and familiar driving behavior is car following, which involves maintaining a constant headway distance from the vehicle-in-front and adjusting the relative velocity accordingly (**Fig. 20**). In this figure, $v(t)$ is the velocity of the driver's vehicle and $h(t)$ is the headway distance from the vehicle-in-front. The velocity of the vehicle-in-front is $v(t) + \dot{h}(t)$, where $\dot{h}(t)$ is the temporal differential of $h(t)$.

In the study reviewed here, the driver was identified using the driving behavior signals that were observed while the driver was performing a car following task.

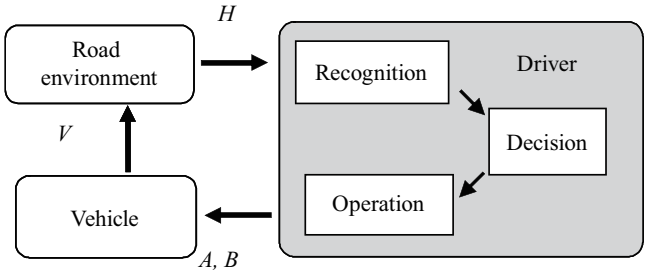

Fig. 19 Basic dynamics of driving behavior, vehicle status, and road environment (A: the force on the acceleration pedal, B: the force on the brake pedal, V: the velocity, H: the headway distance from the vehicle in front).

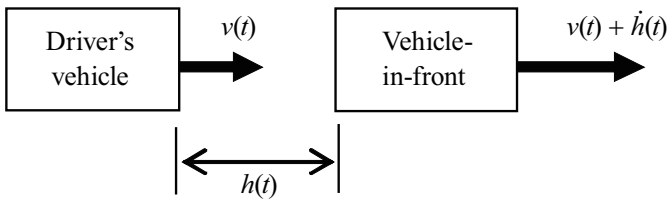

Fig. 20 Car following model. ($v(t)$: the velocity, $h(t)$: the headway distance from the vehicle in front, $\dot{h}(t)$: time differentiation of h).

6. 2 Model Comparison

Two different strategies were compared for driver identification based on driving behavior signals. In the first approach, a physical driving model was used for characterizing the driving in a parametric manner; i.e., the parameters of the dynamic system were used to characterize the driver. For the physical model of car following, the Helly model[32] and optimal velocity model[33] were used, since these two models are frequently used in a wide range of applications.[34,35]

In contrast, in the second method, the driver's characteristics were represented by the distributions of the signals based on a Gaussian mixture model (GMM). In the GMM approach, by estimating the joint distributions of the signals and their time derivatives, both static and dynamic properties of the signals can be modeled implicitly.

6. 2. 1 Parametric Approach: Helly Model

The most familiar model for car following is the stimulus-response model. A difference in the velocity of the vehicle-in-front, as well as a change in the headway distance from that vehicle, stimulates the driver, who responds by either accelerating or decelerating. The Helly model is shown in Eq. (12).

$$\dot{v}(t+T) = C_1\dot{h}(t) + C_2\{h(t) - D\}, \tag{12}$$

where C_1 and C_2 are the response sensitivity to the stimulus, D is the optimum headway distance from the vehicle-in-front, and T is the response delay. These values may be constants or the functions of other variables. While many models had been proposed to represent C_1, C_2, D, and T, the Helly model shown in Eq. (13) was used.

$$\dot{v}(t+T) = \beta_1\dot{h}(t) + \beta_2 h(t) + \beta_3 v(t) + \beta_4, \tag{13}$$

where T, β_1, β_2, β_3, *and* β_4 are constants. As this is a linear model, the parameter estimation is stable and the physical meanings of these parameters can be interpreted easily.

The experiment was performed using a driving simulator. Eight subjects drove two different roads four times each (for total of eight sessions per participant). For the parameter T, a value of 500 ms was used, which was derived from another simple stimulus-response

experiment.

The driver identification method was as follows.

(i) Parameter vector $\boldsymbol{x} = (\beta_1, \beta_2, \beta_3, \beta_4)'$ is calculated for the data obtained from each session, using the least-square-error method.

(ii) For each driver c, the data obtained from the eight sessions was divided into six blocks of learning data and two blocks of estimation data.

(iii) For each driver c, the average parameter vector $\boldsymbol{\mu}_c$ and the covariance matrix $\boldsymbol{\Sigma}_c$ are calculated using the parameter vectors x of the six blocks of learning data.

(iv) For each block of estimation data, the Mahalanobis distance D_c between the estimation data and the average for each driver was calculated. The estimation data is identified as the driver having the least Mahalanobis distance.

$$D_c = (x + \boldsymbol{\mu}_c)' \boldsymbol{\Sigma}_c^{-1} (x + \mu_c) \tag{14}$$

A cross-validation test with the process above gave an identification rate of 43.8%.

6. 2. 2 Parametric Approach: Optimal Velocity Model

Another model that could be applied to the car following task was the optimal velocity model. This model assumes that each driver has a preferred optimal velocity for a given headway distance from the vehicle-in-front. Thus, drivers can be identified by their pattern of acceleration and deceleration according to the difference between the current and optimal velocity.

$$\dot{v}(t + T) = \alpha\{V_{opt}(h(t)) - v(t)\}, \tag{15}$$

$$V_{opt}(h) = V_{max}[1 - exp\{-\alpha(h - h_0)\}], \tag{16}$$

where $V_{opt}(h)$ is the optimal velocity function, α is the sensitivity parameter, V_{max} is the maximum velocity, and a and h_0 are parameters that represent the driver's optimal velocity property. For the parameters T and V_{max}, 500 ms and 32 m/s, respectively, were used; these were derived from another simple experiment. An example of an optimal velocity model is shown in **Fig. 21**(a).

The identification method was the same as that described in Sec. 6. 2. 1, and the identification rate was found to be 54.7%.

6. 2. 3 GMM Approach

Model

GMM is a statistical model that is a linear combination of Gaussian basis functions, and it has many applications.[36] The output probability of GMM λ to the observation vector $\boldsymbol{o}$ is as follows:

$$b(\boldsymbol{o}|\lambda) = \sum_{m=1}^{M} \omega_m N_m(\boldsymbol{o}), \tag{17}$$

$$\lambda = \{\omega_m, \boldsymbol{\mu}_m, \boldsymbol{\Sigma}_m | m = 1, 2, ..., M\}, \tag{18}$$

where $\boldsymbol{o}$ is an observation vector, λ is a GMM, $b(\boldsymbol{o}|\lambda)$ is an output probability, M is the number of mixture functions, $\boldsymbol{\mu}_m$ is the centroid vector of the mth mixture function, $\boldsymbol{\Sigma}_m$ is the covariance matrix of the mth mixture function, and ω_m is the mixture weight for the mth mixture function and satisfies the following equation:

$$\sum_{m=1}^{M} \omega_m = 1. \tag{19}$$

$N_m(\boldsymbol{o})$ is the mth mixture function and is defined by the following equation:

$$N_m(\boldsymbol{o}) = \frac{1}{\sqrt{(2\pi)^D |\boldsymbol{\Sigma}_m|}} \cdot exp\left\{-\frac{1}{2}(\boldsymbol{o} - \boldsymbol{\mu}_m)' \boldsymbol{\Sigma}_m^{-1} (\boldsymbol{o} - \boldsymbol{\mu}_m)\right\}, \tag{20}$$

where $\boldsymbol{\Sigma}_m$ and $\boldsymbol{\Sigma}_m^{-1}$ are the covariance matrix and the inverse of the covariance matrix, respectively; $(\boldsymbol{o} - \boldsymbol{\mu}_m)'$ is the transpose of $(\boldsymbol{o} - \boldsymbol{\mu}_m)$; and D is the dimensionality of $\boldsymbol{o}$. In this work, a diagonal matrix was used for $\boldsymbol{\Sigma}_m$. The likelihood of the model λ to the observation vectors $\boldsymbol{O} = (\boldsymbol{o}_1, \boldsymbol{o}_2, ...)$ is defined by

$$P(\boldsymbol{o}|\lambda) = \prod_{t=1}^{T} b(\boldsymbol{o}_t) = \prod_{t=1}^{T} \sum_{m=1}^{M} \omega_m N_m(\boldsymbol{o}_t). \tag{21}$$

The experimental data were the same as those described in Sec. 6. 2. 1. The identification method was

as follows:

(i) For each driver c, the eight sets of session data are divided into six blocks of learning data and two blocks of estimation data.

(ii) For each driver c, GMM λ_c was estimated. The mixture weight ω_m, centroid vector $\boldsymbol{\mu}_m$, and covariance matrix $\boldsymbol{\Sigma}_m$ are calculated using feature vectors $\boldsymbol{o}$ of six blocks of learning data with the EM algorithm. The elements of the feature vector are some of v, Δv, h, and Δh, where Δx represents the temporal change in value x and is calculated using the following equation:

$$\Delta x(t) = \frac{\sum_{k=-K}^{K} k x(t+k)}{\sum_{k=-K}^{K} k^2} \quad . \tag{22}$$

Here, $x(t)$ is the original feature and K is the time window duration ($2K$ = 600 ms). The mixture number is 2, 4, 8, or 16.

(iii) For each block of estimation data, the likelihood $P(\boldsymbol{O}|\lambda_c)$ for each driver c was calculated. The estimation data are associated with the driver for whom the likelihood is highest.

An example GMM is shown in Fig. 21(b). A cross-validation test was done using the above process.

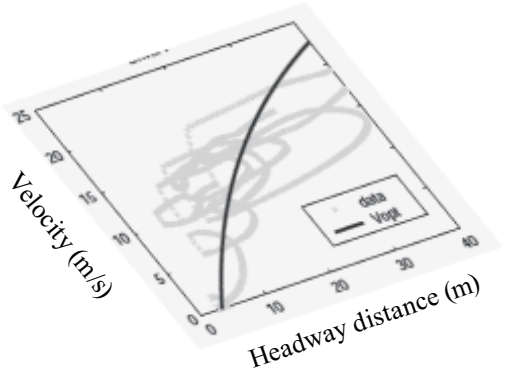

(a) An example of the optimum velocity model. A gray line represents a driving behavior signal of a driver. The black line represents the optimal velocity model calculated from the driving behavior signals of the driver.

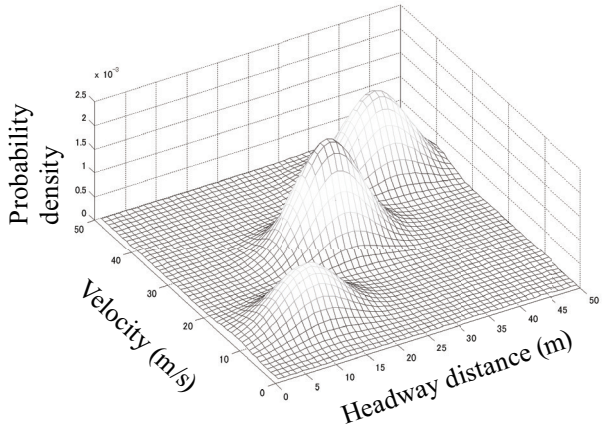

(b) An example of the GMM model calculated from the same signals of (a). The height represents the output probability distribution of the GMM model.

Fig. 21 Examples of a physical model and a statistical model.

Results

The identification results are shown in **Fig. 22**, where V is the velocity, H is the headway distance from the vehicle-in-front, and Δ represents the temporal change. Modeling the dynamics of the driving signals is also important in the GMM approach.[37] The best identification rate was 78%, which was obtained using V, ΔV, H, and ΔH.

The Helly model described in Sec. 6. 2. 1 used the variables v, $\dot{v}$, h, and $\dot{h}$, and the identification rate was 43.8%. The identification rate of GMM using similar features V, ΔV, H, and ΔH was 78%. The optimal velocity model described in Sec. 6. 2. 2 used the variables v, $\dot{v}$, and h, and the identification rate was 54.7%. The identification rate of GMM using fewer features V and H was 69%. In each case, the GMM model was found to be better than the parametric physical model. This result suggests that:

- GMM can be used to represent the underlying dynamics between features with the joint distribution function.
- GMM can represent the non-linearity and the stochastic aspects with a probabilistic distribution function.

6. 3 Feature Comparison for GMM

The features of GMM were compared using actual driving behavior data from 30 drivers.[38] The average duration of driving data acquisition for each driver was around 20 min. The first 10 min was used for training and the remaining 10 min for testing.

Figure 23 shows the identification rates using

a single feature and multiple features. In the figure, *A*, *B*, *V*, and *Δ* indicate the force on the accelerator pedal, the force on the brake pedal, the vehicle speed, and the dynamics, respectively.

The feature combination *AΔA* provided the highest performance. The fact that accelerator pedal force was the best driver identifier could be interpreted as follows:

- As the accelerator pedal is operated directly by the driver, it is best at preserving individual behavior.
- Since the brake pedal is operated less frequently than the accelerator pedal, its identification performance is low.
- The vehicle velocity *V* and the headway distance from the vehicle-in-front *H* are obtained by the convolution of the driver's operation, the physical properties of the vehicle, and the properties of the vehicle-in-front (Fig. 19). As a result, personal information is obscured by the inclusion of *V* and *H*.

To improve the identification rate, the features of the accelerator pedal and brake pedal were combined. As drivers cannot press both pedals simultaneously, the joint distribution of the force on the accelerator pedal and the force on the brake pedal has no effect. Thus, the sum of the log-likelihood of the force on both the accelerator and brake pedals was used. **Figure 24** shows the result. The highest identification rate of 73% was obtained using *AΔA* + *BΔB*.

In this section, both physical and statistical models were reviewed, and the statistical models were found to out-perform the physical models. Also, interpretation of the physical meaning was found to be effective for feature and model selection in the statistical models.

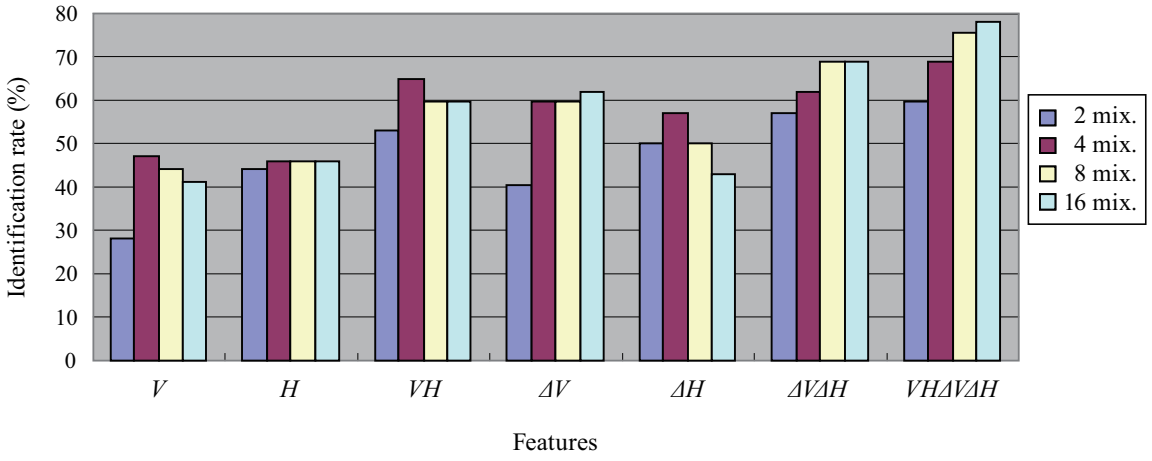

Fig. 22 Driver identification rate of GMM with various number of mixtures (*V*: velocity, *H*: headway distance, *ΔV*: temporal change of *V*, *ΔH*: temporal change of *H*).

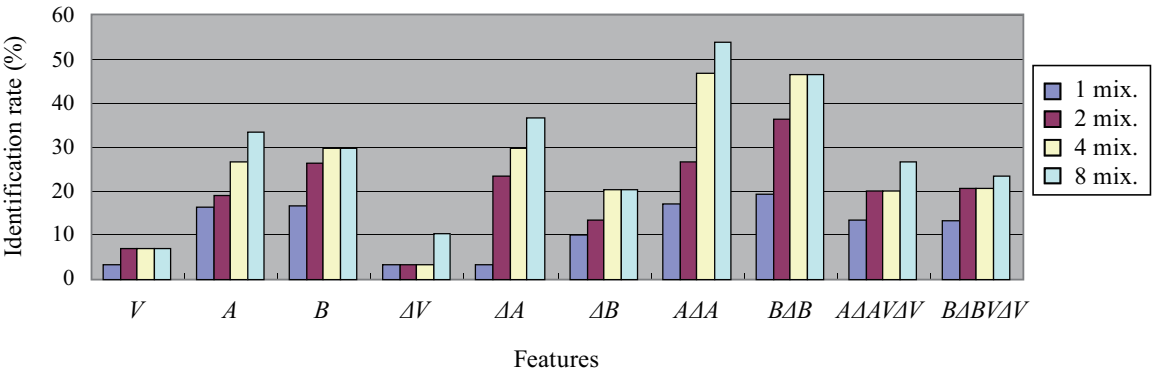

Fig. 23 Driver identification rate of GMM for driving signals of actual vehicles (*A*: the force on the acceleration pedal, *B*: the force on the brake pedal, *V*: the velocity, *Δ*: temporal change).

7. Discussion

In this section, the modeling studies covered by this review are summarized.

Regarding sound evaluation (Sec. 3), a hearing model commonly used in psychophysics was used to analyze human hearing. The model clarified the rumble sound features that are consistent with human hearing. This research resulted in an objective evaluation model.

In Sec. 4, an evaluation index of the human-machine interface in information equipment operation was developed by applying the keystroke-level model, which is widely used in cognitive science. Using this model, the human operation process could be structured and the task times could be predicted. The study could concentrate on expanding the model to other driving matters (e.g., the division of glances).

Regarding drowsiness detection (Sec. 5), despite extensive study, precise drowsiness index that can estimate the reaction delay and that can be measured onboard had been unknown. To develop a useful index, it was necessary to clarify the relationships among drowsiness, reaction delay, and measurement features. fMRI measurements and statistical analysis revealed that drowsiness and reaction delay were caused by decreased activity in the brainstem. Based on the neural model of eye movement triggered by the brainstem, SEM was found to be a precise index.

Finally, in Sec. 6, a study to improve driver identification based on statistical human behavior models was reviewed; conventional physical models were good but not precise enough for real human behavior. The statistical models, which out-performed the physical models, used features similar to the temporal features of the physical models. This suggested that the statistical model could relax the rigid relationship among features described using differential equations. These relaxations are suitable for stochastic, context-dependent, individually different, and nonlinear human characteristics. Interpreting the physical meaning was effective for feature selection, model selection, and application of the statistical model results.

In general, multiple models exist for each human characteristic. The application of physical models ranges from microscopic cells to macroscopic social behaviors. The complexity of statistical models ranges from simple linear regressions to large convolutional neural networks. Also, model structure and learning algorithms have many variations. To use these models, it is important to choose a model that is sufficient for the design being evaluated and appropriate for the amount of data available. Complex models are not necessarily better than simple models. In many cases, the simplest model that describes the actual data has the best performance.[39]

In the near future, research on human characteristics is expected to make great progress. One direction is generic model research. As shown in this paper, although there are many types of human models, a common base principle or common fundamental equation does not exist. Therefore, the research results

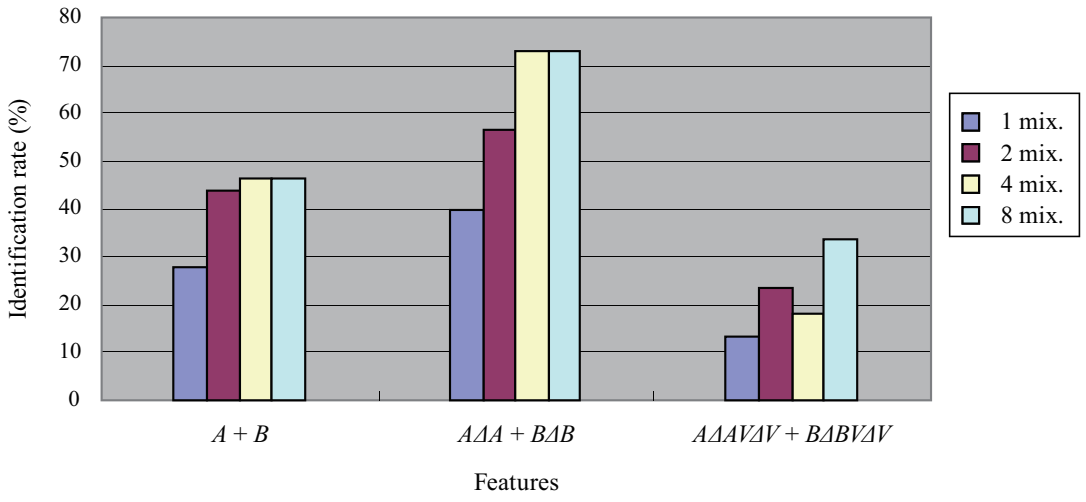

Fig. 24 Driver identification rate of multiple likelihood of actual vehicles (A: the force on the acceleration pedal, B: the force on the brake pedal, V: the velocity, Δ: temporal change).

are sometimes hard to accumulate and share among different research domains. Recently, the free energy principle was proposed as a unified brain principle[40] and applied to various human characteristics.[41] These directions are expected to help human characteristics research evolve from case studies to systematic research.

Another direction is the whole-brain model research, which attempts to develop a functional model of the entire brain, including cognition, speculation, memory, learning, emotion, and consciousness. Some research groups are trying to simulate all neurons of a brain,[42] while others are trying to develop generic artificial intelligence software.[43] These studies are expected to provide a systematic perspective for human characteristics research.

Through these studies and advances in data science and large-scale data accumulation, it is expected that human model-based designs for automobiles will evolve rapidly.

References

(1) Kawasumi, M., "Measurement of Color Discrimination Ellipse for Object's Surface with Texture" (in Japanese), *R&D Review of Toyota CRDL*, Vol. 34, No. 1 (1999), p. 94.

(2) Wakita, T. et al., "Objective Rating of Rumble in Vehicle Passenger Compartment During Acceleration", *SAE 1989 Transactions, Journal of Passenger Cars*, Section 6, Vol. 98 (1989), pp. 1162-1169, SAE International.

(3) Inagaki, H. et al., "Evaluation of Seat Kansei Quality" (in Japanese), *R&D Review of Toyota CRDL*, Vol. 35, No. 4 (2000), pp. 9-14.

(4) Sato, S., "Air Quality in a Car's Cabin" (in Japanese), *R&D Review of Toyota CRDL*, Vol. 33, No. 4 (1998), pp. 15-23.

(5) Doi, S., "Recent and Future Trends of Driving Performance Evaluation" (in Japanese), *J. Soc. Automot. Eng. Jpn.*, Vol. 58, No. 12 (2004), pp. 4-9.

(6) National Highway Traffic Safety Administration, "Driver Distraction: A Review of the Current State-of-knowledge", No. DOT HS 810 787 (2008).

(7) Uchiyama, Y. et al., "Voice Information System Adapted to Driver's Mental Workload", *Proc. Hum. Factors Ergon. Soc. Annu. Meet.* (2002), pp. 1871-1875.

(8) Kurahashi, T. et al., "Analysis of Normal Drivers' Braking Timing on Public Roads" (in Japanese), *Trans. JSAE*, Vol. 38, No. 6 (2007), pp. 247-252.

(9) Abbink, D. A. et al., "Haptic Shared Control: Smoothly Shifting Control Authority?", *Cong. Tech. Work*, Vol. 14, No. 1 (2012), pp. 19-28.

(10) Hastie, T. et al., *The Element of Statistical Learning: Data Mining, Inference and Prediction* (2001), 533p., Springer.

(11) Andrews, S. A. et al., *Analysis and Mechanism of Engine Crank Rumble* (1979), pp. 99-109, I Mech E Conf. Publ.

(12) Tsuge, K. et al., "A Study of Noise in Vehicle Passenger Compartment During Acceleration", *SAE Tech. Pap. Ser.*, No. 850965 (1985).

(13) Zwicker, E., "Subdivision of the Audible Frequency Range into Critical Bands", *J. Acoust. Soc. Am.*, Vol. 33, No. 2 (1961), p. 248.

(14) Wakita, T. et al., "Objective Evaluation Method of In-vehicle Information System Usability", *IPSJ Journal* (in Japanese), Vol. 42, No. 7 (2001), pp. 1762-1769.

(15) Urokohara, H. et al., "A Usability Evaluation Method That Compare Task Performance Between Expert and Novice", *Human Interface Symp.* (in Japanese) (1999), pp. 537-542.

(16) Zwahlen, H. T. et al., "Safety Aspects of CRT Touch Panel Controls in Automobiles", *Vision in Vehicles II* (1988), pp. 335-344, North-Holland.

(17) Ito, T. et al., "Japan's Safety Guideline on In-vehicle Display Systems", *Proc. 4th World Congr. on ITS* (1997), ITS.

(18) Kimura, K. et al., "In-vehicle Navigation System Operability While Driving", *Proc. 6th World Congr. on ITS* (1999), ITS.

(19) Miyake, S. et al., "Subjective Mental Workload Assessment Technique: An Introduction to NASA-TLX and Swat and a Proposal of Simple Scoring Methods", *Jpn. J. Ergon.* (in Japanese), Vol. 29, No. 6 (1993), pp. 399-408.

(20) Japan Safe Driving Center, "Research about the Relationship Between the Driving Behavior and the Mobile Phone Usage", *Research Report* (in Japanese), (1997), 327p.

(21) Ito, T. et al., "Jama's Activity on In-vehicle Information System's Safety No. 2", *Symp. Socio Ergon. Human Interface of Mobile Phone and Car Navi.* (in Japanese) (2000), pp. 75-80, Japan Ergonomics Society.

(22) Kojima, S. et al., "Development of an Evaluation Method for Verbal Interface in Driving", *IPSJ SIG Notes* (in Japanese), Vol. 99, No. ITS-3 (1999), pp. 71-75.

(23) Card, S. et al., *The Psychology of Human-computer Interaction* (1983), 469p., Lawrence Erlbaum Associates.

(24) Uchiyama, Y. et al., "Decreased Thalamus and Brainstem Baseline Brain Activity Relates to Reaction Delays in a Drowsy State", *Proc. JSAE Annu. Congr.* (in Japanese), No. 121-11 (2011), pp. 19-22, JSAE.

(25) Sakai, H. et al., "Slow Eye Movement as a Possible Predictor of Reaction Delays to Auditory Warning Alarms in a Drowsy State", *Ergonomics*, Vol. 54, No. 2 (2011), pp. 146-153.
(26) Wierwille, W. W. and Ellsworth, L. A., "Evaluation of Driver Drowsiness by Trained Raters", *Accident Analysis & Prevention*, Vol. 26, No. 5 (1994), pp. 571-581.
(27) Krvklunf, G. and Akerstedt, T., "Sleepiness in Long Distance Truck Driving: An Ambulatory EEG Study of Night Driving", *Ergonomics*, Vol. 36, No. 9 (1993), pp. 1007-1017.
(28) Saper, C. B. et. al., "Hypothalamic Regulation of Sleep and Circadian Rhythms.", *Nature*, Vol. 437, No. 7063 (2005), pp. 1257-1263.
(29) Kinomura, S. et al., "Activation by Attention of the Human Reticular Formation and Thalamic Intralaminar Nuclei", *Science*, Vol. 271 (1996), pp. 512-515.
(30) Gancarz, G. and Grossberg, S., "A Neural Model of the Saccade Generator in the Reticular Formation", *Neural Networks*, Vol. 11 (1998), pp. 1159-1174.
(31) Helly, W., "Simulation of Bottlenecks in Single Lane Traffic Flow", *Proc. Symp. on Theory of Traffic Flow* (1959), pp. 207-238, Research Laboratories, General Motors.
(32) Wakita, T. et al., "Driver Identification Using Driving Behavior Signals", *IEICE Trans. Inf. & Syst.*, Vol. E89-D, No. 3 (2006), pp. 1188-1194.
(33) Oguchi, T., "Analysis of Bottleneck Phenomena at Basic Freeway Segments: Car-following Model and Future Exploration" *Proc. JSAE* (in Japanese), Vol. 660, IV-49, (2000), pp. 39-51, JSAE.
(34) Brackstone, M. and McDonald, M., "Car-following: A Historical Review", *Transportation Research Part F*, Vol. 2, No. 4 (1999), pp. 181-196.
(35) Ranjtkar, R. et al., "Performance Evaluation of Microscopic Traffic Flow Models with Test Track Data", *Proc. TRB Annu. Meet.,* Vol. 1876 (2004), pp. 90-100, TRB.
(36) Reynolds, D. A. and Rose, R. C., "Robust Text-independent Speaker Identification Using Gaussian Mixture Speaker Models", *IEEE Trans. Speech and Audio Processing*, Vol. 3, No. 1 (1995), pp. 72-83.
(37) Furui, S., "Speaker-independent Isolated Word Recognition Using Dynamic Features of Speech Spectrum", *IEEE Trans. Acoust. Speech Signal Processing*, Vol. 34, No. 1 (1986), pp. 52-59.
(38) Kawaguchi, N. et al., "Multimedia Data Collection of In-car Speech Communication", *Proc. European Conf. Speech Commun. Technol.* (Eurospeech) (2001), pp. 2027-2030, ISCA.
(39) Rissanen, J., "Modeling by Shortest Data Description", *Automatica*, Vol. 14, No. 5 (1978), pp. 465-471.
(40) Friston, K., "The Free-energy Principle: A Rough Guide to the Brain?", *Trend of Cognitive Sciences*, Vol. 13, No. 7 (2009), pp. 293-301.
(41) Seth, A., "The Cybernetic Bayesian Brain", *Open MIND* (2015), pp. 1410-1433, <https://open-mind.net/collection.pdf>, (accessed 2017-09-01).
(42) Kanzaki-Takahashi Laboratory, "From the Insect Brain to the Bio-mechanic System", *Research Interest*, <http://www.brain.imi.i.u-tokyo.ac.jp/research/interest_eng.html>, (accessed 2017-09-01).
(43) Wole Brain Archtecture Initiative, "Whole Brain Architecture Initiative", *Let's Build a Brain Together*, <https://wba-initiative.org/en/>, (accessed 2017-09-01).

Toshihiro Wakita

Research Field:
- Human Factors

Academic Degree: Ph.D.

Academic Societies:
- IEEE
- Society of Automotive Engineers of Japan
- The Institute of Electronics, Information and Communication Engineers

